Control of a flexible beam actuated by macro-fiber composite patches: II. Hysteresis and creep compensation, experimental results

authored by **J. Schröck, T. Meurer, and A. Kugi**

and published in *Smart Materials and Structures*.

Contact:

Automation and Control Institute (ACIN)
Vienna University of Technology
Gusshausstrasse 27-29/E376
1040 Vienna, Austria

Internet: www.acin.tuwien.ac.at
E-mail: office@acin.tuwien.ac.at
Phone: +43 1 58801 37601
Fax: +43 1 58801 37699

Control of a flexible beam actuated by macro-fiber composite patches - Part II: Hysteresis and creep compensation, experimental results

J. Schröck, T. Meurer, A. Kugi

Automation & Control Institute, Gußhausstr. 27-29, 1040 Vienna, Austria

E-mail: schroeck@acin.tuwien.ac.at

Abstract. This paper considers a flexible cantilever beam, which is actuated by piezoelectric macro-fiber composite (MFC) patch actuators. For accurate positioning tasks, special attention has to be paid to the inherent nonlinear hysteresis and creep behavior of these actuators. A detailed analysis of the MFC-actuated cantilever verifies that these nonlinearities can be efficiently captured by an operator-based model using Prandtl-Ishlinskii's theory. Based on a Hammerstein-like model with the nonlinearities at the input connected in series with a linear infinite-dimensional beam model it follows that hysteresis and creep effects can be compensated by application of the inverse operator. Experimental results prove the feasibility of this approach. With this result the tracking accuracy of the combination of the compensator with the flatness-based feedforward control design as proposed in the companion paper [1] can be verified. Measurements demonstrate the applicability of this approach for the realization of highly dynamic trajectories for the beam's tip deflection.

Submitted to: *Smart Material and Structures*

Post-print version of the article: J. Schröck, T. Meurer, and A. Kugi, "Control of a flexible beam actuated by macro-fiber composite patches: II. Hysteresis and creep compensation, experimental results", *Smart Materials and Structures*, vol. 20, no. 015016, pp. 1–10, 2011.
DOI: 10.1088/0964-1726/20/1/015016

1. Introduction

Piezoelectric ceramics is a very popular material in the field of actuator and sensor technology because of its large bandwidth, fast response time and the ability to generate high forces. However, since the displacements of piezoelectric actuators are rather limited their main application areas are focused on micro-positioning devices and vibration suppression. In some applications, piezoelectric patches are bonded on or embedded in flexible lightweight structures, thus providing smart structures with intrinsic sensing and actuating capabilities. In this context, PZT (lead zirconate titanate) is one of the most widely used piezoelectric material. Due to the very brittle nature of PZT patches the structure is locally significantly stiffened such that the original flexibility of the lightweight construction is drastically reduced. This drawback can be eliminated by the use of macro-fiber composite (MFC) patch actuators. These patch actuators are composed of rectangular piezoceramic fibers embedded in an epoxy matrix and covered by interdigitated electrodes on both sides of the patch. This configuration results in a very flexible patch. Additionally, the large input voltage range $[-500, +1500]$ V together with a larger electromechanical coupling coefficient compared to conventional PZT patches allow for higher actuation forces and larger displacements [2].

However, it is well known that active materials, like magneto- and electrostrictive materials, shape memory alloys as well as piezoelectric materials, show intrinsic hysteretic behavior and creep effects [3], [4]. Especially in the case of positioning tasks, where the full range of the input voltage has to be used in order to realize large displacements, these nonlinear effects cannot be neglected. Since the systematic consideration of hysteresis and creep behavior in the formulation of the constitutive relations of piezoelectric materials is still an open question most attempts in dealing with these nonlinearities are based on phenomenological approaches [5], [6]. In this contribution, the nonlinear MFC-actuated beam structure is represented in the form of a Hammerstein-like model consisting of a serial connection of the nonlinear hysteretic and creep model and a linear infinite-dimensional beam model (see [7] for related results for a PZT parallel trimorph bender). A very efficient way for modeling these nonlinearities are the Preisach and the Prandtl-Ishlinskii operator approach [6], [8]. Due to the Hammerstein-like structure the appropriate inverse operator yields the hysteresis and creep compensator that annihilates the nonlinear behavior of the MFC actuators. In order to exploit the pleasant property of the analytic invertibility of the Prandtl-Ishlinskii operator the actuator nonlinearities have to show certain characteristics. However, a detailed analysis of the actuator behavior verifies the application of the Prandtl-Ishlinskii approach in case of the MFC-actuated cantilever shown in figure 1. This configuration of a flexible beam with piezoelectric patch actuators is also investigated in the companion paper [1]. Therein, the motion planning and feedforward control problem is systematically solved based on a linear infinite-dimensional system description. In this contribution it is shown by experimental results that combining the

Post-print version of the article: J. Schröck, T. Meurer, and A. Kugi, "Control of a flexible beam actuated by macro-fiber composite patches: II. Hysteresis and creep compensation, experimental results", *Smart Materials and Structures*, vol. 20, no. 015016, pp. 1–10, 2011.
DOI: 10.1088/0964-1726/20/1/015016

flatness-based feedforward controller with the hysteresis and creep compensator allows to realize the accurate tracking of highly dynamic trajectories for the beam's tip deflection without the excitation of spurious oscillations.

The paper is organized as follows: In Section 2, a detailed analysis of the nonlinear MFC actuator behavior is presented followed by an operator based modeling approach of the hysteresis and creep effects. Section 3 discusses the compensator design which is verified by measurements in Section 4. The experimental results are twofold. On the one hand, it is shown that the proposed compensator allows to cancel the hysteresis and creep behavior of the MFC patches and on the other hand the feasibility of the feedforward control design proposed in [1] is validated by means of measurements.

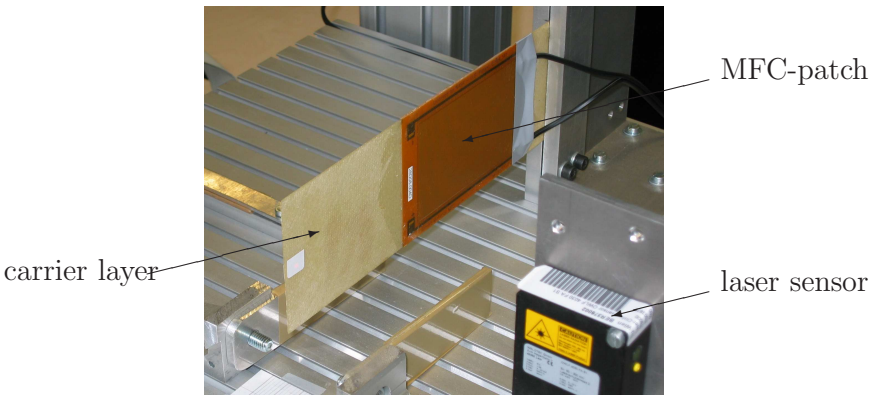

Figure 1. Piezo-actuated flexible beam.

2. Analysis and modeling of the actuator behavior

In the following, a cantilevered rectangular flexible beam with one pair of MFC patch actuators is considered, see figure 1. By application of an asymmetric voltage supply the deflection of the beam is restricted to a pure bending motion. This means the voltage applied to the patch on the front side of the beam $\overline{u}^{fs}(t)$ and the voltage applied to the patch on the back side of the beam $\overline{u}^{bs}(t)$ are given by

$$\overline{u}^{fs}(t) = u_0 + u(t) \text{ and } \overline{u}^{bs}(t) = u_0 - u(t), \tag{1}$$

respectively. Here, the constant supply voltage $u_0 = (u_{max} + u_{min})/2$ is used to enable a balanced voltage supply $u(t) \in [-\frac{u_{max}+|u_{min}|}{2}, +\frac{u_{max}+|u_{min}|}{2}]$, whereas $u_{min} = -500$ V and $u_{max} = 1500$ V are the actuator specific minimal and maximal supply voltages. In order to achieve large displacements of the beam's tip the whole input voltage range of the MFC patch actuators has to be utilized. However, the typical large-signal behavior of piezoelectric materials shows significant hysteretic nonlinearities and creeping effects that cannot be neglected. Therefore, the nonlinear behavior of MFC patch actuators is analyzed prior to the design of an appropriate hysteresis and creep compensator.

Post-print version of the article: J. Schröck, T. Meurer, and A. Kugi, "Control of a flexible beam actuated by macro-fiber composite patches: II. Hysteresis and creep compensation, experimental results", *Smart Materials and Structures*, vol. 20, no. 015016, pp. 1–10, 2011.
DOI: 10.1088/0964-1726/20/1/015016
The content of this post-print version is identical to the published paper but without the publisher's final layout or copy editing.

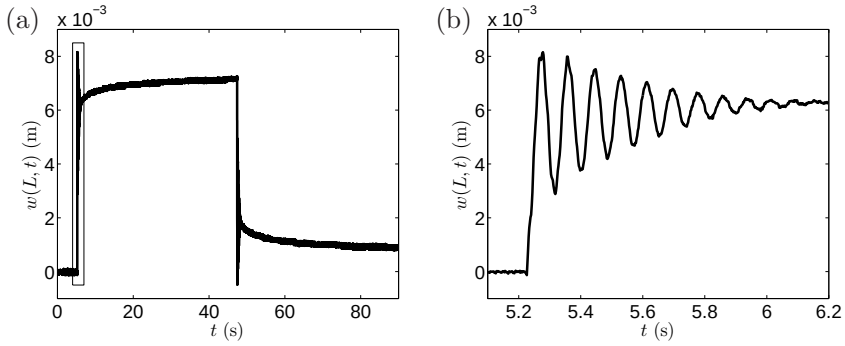

Figure 2. (a) Response of the beam's tip deflection due to a rectangular voltage signal of 500V. (b) Detailed view of the time interval $[5.1, 6.2]$ s.

2.1. Nonlinear behavior of MFC patch actuators

According to [6] a hysteretic nonlinearity is a causal and rate-independent relation with memory effect between an input signal u and an output signal y. Here the term memory indicates that the output depends not only on the present value of the input but also on the evolution of the input in the past. The notation of creep originates from the field of solid mechanics and describes a rate-dependent deformation behavior as shown by visco-plastic and viscoelastic materials.

Both nonlinearities, hysteresis as well as creep, are fairly developed in the behavior of MFC actuators. Figure 2 depicts the measured response of the beam's tip deflection due to a rectangular voltage signal with the amplitude $u = 500$ V in the time interval $t \in [5, 45]$. After the decay of the transient behavior significant creep effects can be observed. By comparing the beam's tip deflection at $t = 0$ s and $t = 90$ s it can be seen that there remains an offset of approximately 1 mm after the creeping comes to a rest. Application of a smooth staircase voltage signal between -500 V and 1500 V, as depicted in figure 3 (a), results in the beam's tip deflection illustrated in figure 3 (b). By combining these measurements as shown in figure 3 (c), where the tip deflection is plotted over the applied voltage signal, the formation of a hysteretic loop can be observed. Additionally, creeping becomes visible in terms of the appearing vertical sections, where a change in the beam's tip deflection occurs although the applied voltage remains constant. The latter behavior is also called rate-dependent material behavior with equilibrium hysteresis [9].

At this point it should be mentioned that piezoelectric actuators generally show significantly less hysteretic behavior in the case of charge control [10]. Figure 4 depicts the hysteretic loop of the tip deflection/voltage relation as well as the hysteretic loop of the tip deflection/charge relation, whereas in the latter case the charge is measured by means of a Sawyer-Tower circuit [11]. From this it can be deduced that charge control has the potential to significantly reduce the hysteretic effects of MFC actuators. However, it is well known that in case of charge controlled actuators stationary deflections cannot be achieved due to their inherent leakage behavior. Therefore, in

Post-print version of the article: J. Schröck, T. Meurer, and A. Kugi, "Control of a flexible beam actuated by macro-fiber composite patches: II. Hysteresis and creep compensation, experimental results", *Smart Materials and Structures*, vol. 20, no. 015016, pp. 1–10, 2011.
DOI: 10.1088/0964-1726/20/1/015016
The content of this post-print version is identical to the published paper but without the publisher's final layout or copy editing.

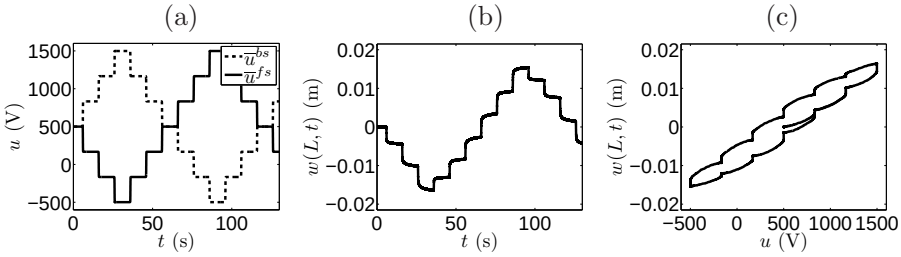

Figure 3. (a) Voltage signals applied to the patch actuator on the front and back side, $\overline{u}^{fs}(t)$, $\overline{u}^{bs}(t)$, respectively, (b) position of the beam's tip $w(L,t)$, (c) hysteresis and creep behavior of the tip deflection/voltage relationship.

practical applications charge control is typically combined with voltage control for the stationary case yielding a so-called hybrid control concept. Another possibility is the application of voltage control with hysteresis and creep compensation. This allows to avoid specialized equipment and thus reduces the complexity and the costs of the control hardware. For this, the systematic design and realization of an operator-based compensator will be presented in the next sections.

2.2. Operator-based modeling

The fact that the tip deflection/charge relation exhibits less nonlinear behavior than the tip deflection/voltage relation as discussed in the preceding section gives rise to the assumption that the main nonlinear effects originate in the charge/voltage relation. Assuming the electric flux density $D^2 = D^3 = 0$, $D^1 = \overline{u}/(e_s\beta_{11})$ [1] and integrating over the effective electrode surface A yields the electric charge

$$\overline{q} = \int_A D^1 \mathrm{d}A = q_0 + \frac{A}{\beta_{11} e_s}\tilde{W}[u] = q_0 + \overline{W}[u], \tag{2}$$

where q_0 reflects the charge due to the constant voltage u_0 in the asymmetric voltage supply (1) and $\tilde{W}$ as well as $\overline{W}$ denote the operators modeling the nonlinear hysteresis and creep effects. Note that due to the symmetric configuration of the piezo-actuated flexible cantilever the hysteresis and creep operator for the patch located at the front side of the beam and the operator for the patch located on the back side of the beam coincide, i.e. $\overline{W}^{fs} = \overline{W}^{bs} = \overline{W}$. This can be verified by means of measurements as depicted in figure 5, where the asymmetric voltage supply (1) is applied to the MFC patch pair. This asymmetric voltage supply is realized by the wiring presented in figure 6, such that only one adjustable voltage source $u(t)$ is required. The electric charge at the connected middle electrodes is given by

$$q = \overline{q}^{fs} - \overline{q}^{bs} = \overline{W}[u] - \overline{W}[-u] = W[u]. \tag{3}$$

Here, the operator W has the property of point symmetry with respect to the origin, i.e. $W[u] = \overline{W}[u] - \overline{W}[-u] = -(\overline{W}[-u] - \overline{W}[u]) = -W[-u]$, what is also confirmed by means of the measurements presented in figure 5.

As shown in the preceding section, the nonlinear behavior of the actuator pair is

Post-print version of the article: J. Schröck, T. Meurer, and A. Kugi, "Control of a flexible beam actuated by macro-fiber composite patches: II. Hysteresis and creep compensation, experimental results", *Smart Materials and Structures*, vol. 20, no. 015016, pp. 1–10, 2011.
DOI: 10.1088/0964-1726/20/1/015016
The content of this post-print version is identical to the published paper but without the publisher's final layout or copy editing.

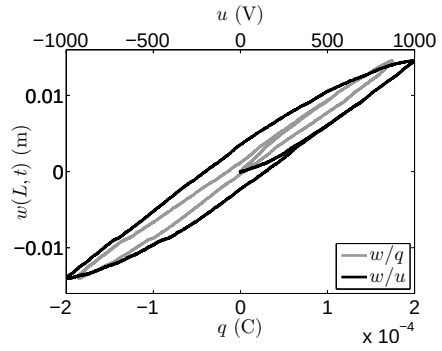

Figure 4. Hysteretic effects in the relation of the beam's tip deflection $w(L,t)$ vs. the actuator voltage $u(t)$ and in the relation of the beam's tip deflection $w(L,t)$ vs. the electric charge of the actuator $q(t)$.

based on hysteresis and creep effects. These effects can be clearly distinguished by their rate-independent and rate-dependent behavior, respectively, such that the operator W can be defined by the superposition of a rate-independent hysteresis operator H and a rate-dependent creep operator C, i.e.

$$q = W[u] = H[u] + C[u], \tag{4}$$

see [12]. With this operator-based hysteresis and creep model the overall system of the MFC-actuated cantilever can be represented in form of a Hammerstein-like model illustrated in figure 7 consisting of the operator $q = W[u]$ at the input connected in series with the linear model of the beam structure. In order to identify the operators H and C the nonlinear behavior of the MFC patch pair is investigated in more detail. The measurements in figure 8 show that, apart from some minor variations, which result from the superposed creeping effects, the hysteretic behavior corresponds to the typical branching behavior also known as Madelung rules [13], [5]:

(i) Any curve c_1 originating at a turning point p_1 of the input-output trajectory is uniquely determined by the coordinates of p_1.

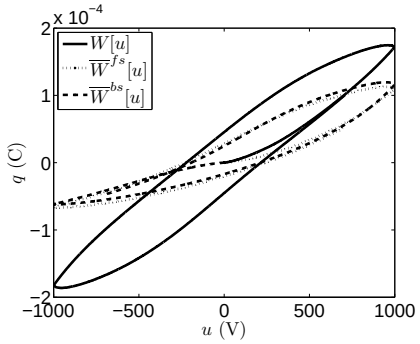

Figure 5. Hysteresis operator of the patch pair W, of the patch at the front side of the beam $\overline{W}^{fs}$, and of the patch at the back side of the beam $\overline{W}^{bs}$.

Post-print version of the article: J. Schröck, T. Meurer, and A. Kugi, "Control of a flexible beam actuated by macro-fiber composite patches: II. Hysteresis and creep compensation, experimental results", *Smart Materials and Structures*, vol. 20, no. 015016, pp. 1–10, 2011.
DOI: 10.1088/0964-1726/20/1/015016

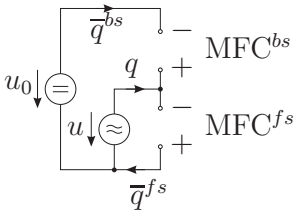

Figure 6. Voltage supply of the MFC patch pair.

(ii) The curve c_2 generated by any turning point p_2 on the curve c_1 leads back to the point p_1 and generates a minor hysteretic loop.

(iii) The continuation of the curve c_2 beyond the point p_1 coincides with the major hysteretic loop and leads back to the point p_1.

Additionally, the measurements in figure 8 (b) illustrate the so-called intersection property [14]. This property states that infinitely many branches can originate from a given point in the input-output plane (e.g. p_3) for a given direction of the input signal. In order to reproduce such intersection effects, the appropriate model of the hysteretic nonlinearity requires an infinite-dimensional memory representation. The best known examples of such systems, which include a so-called global-memory structure, are the Preisach and the Prandtl-Ishlinskii operators. While the Preisach approach allows to model very general hysteretic nonlinearities the Prandtl-Ishlinskii approach considers only hysteretic nonlinearities with odd symmetrical loops. Note that this restriction can be overcome by concatenating the Prandtl-Ishlinskii operator with an asymmetrical memory-free nonlinearity, which results in the so-called modified Prandtl-Ishlinksii operator, see, e.g., [8].

As presented in figure 8, the MFC-actuated flexible beam structure exhibits hysteretic nonlinearities with odd symmetrical loops. Additionally, the Masing rule [5] is fulfilled, i.e. input signals that vary between relative extrema of arbitrary but fixed amplitudes generate congruent minor hysteretic loops. Thus all requirements are fulfilled to use the Prandtl-Ishlinskii approach for the modeling of the hysteretic effects of the MFC patch pair.

A detailed investigation of the creeping effect shows a clear correspondence to $\log(t)$-creep behavior. This is shown in figure 9 (b), where the transition phases of the beam's tip deflection, which result from the application of a smooth staircase voltage signal

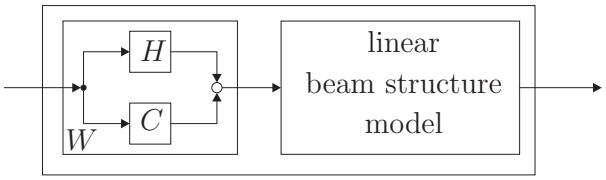

Figure 7. Hammerstein-like model of MFC-actuated beam structure

Post-print version of the article: J. Schröck, T. Meurer, and A. Kugi, "Control of a flexible beam actuated by macro-fiber composite patches: II. Hysteresis and creep compensation, experimental results", *Smart Materials and Structures*, vol. 20, no. 015016, pp. 1–10, 2011.
DOI: 10.1088/0964-1726/20/1/015016
The content of this post-print version is identical to the published paper but without the publisher's final layout or copy editing.

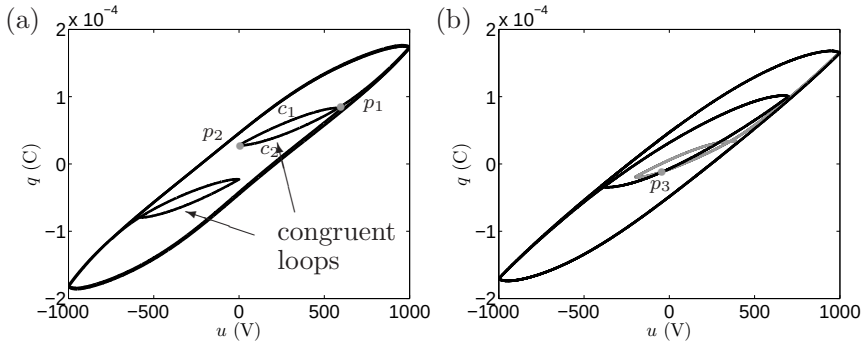

Figure 8. (a) Madelung and Masing rule, (b) Intersection property.

according to figure 9 (a), are plotted over a logarithmic time axis. The varying slopes of the lines in figure 9 (b) indicate that the creep behavior depends on the evolution of the voltage signal in the past. This memory effect can also be modeled by the global-memory structure of a Prandtl-Ishlinskii operator [12].

3. Compensator design

Due to the special structure of the operator-based model (4) it is obvious that a compensator based on the inverse operator W^{-1}, which is defined by

$$W^{-1}[W[u]] = u, \tag{5}$$

annihilates the hysteresis and creep behavior of the actuator pair and ensures a linear input-output behavior. As mentioned in the preceding section the Prandtl-Ishlinskii approach as well as the Preisach approach represent both adequate possibilities for modeling the analyzed behavior. However, the determination of the inverse Preisach operator can be performed only numerically and requires a high computational effort while the Prandtl-Ishlinskii approach allows an analytical solution for the inverse operator. This property is of great advantage in view of real-time implementation.

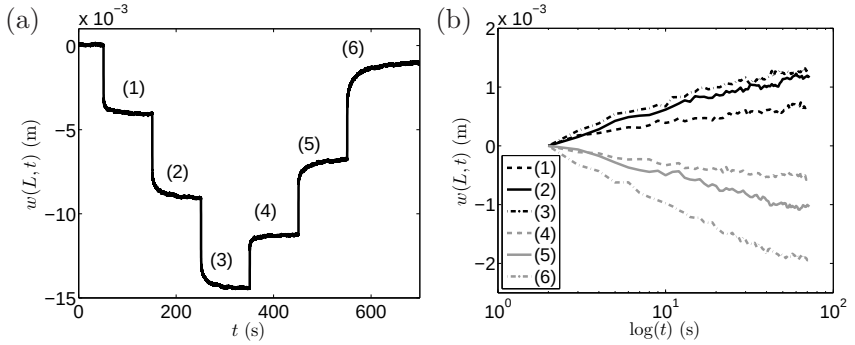

Figure 9. Creep behavior shown by measurements of the beam's tip deflection. (a) Trajectory of the beam's tip, (b) transition phases (1)-(6) depicted over a logarithmic time axis.

Post-print version of the article: J. Schröck, T. Meurer, and A. Kugi, "Control of a flexible beam actuated by macro-fiber composite patches: II. Hysteresis and creep compensation, experimental results", *Smart Materials and Structures*, vol. 20, no. 015016, pp. 1–10, 2011.
DOI: 10.1088/0964-1726/20/1/015016

3.1. The Prandtl-Ishlinskii approach

In the following, the hysteresis and creep model with an input signal $\upsilon(t)$ and an output signal $\varsigma(t)$ is defined by

$$\varsigma(t) = H[\upsilon](t) + C[\upsilon](t) = W[\upsilon](t), \tag{6}$$

with the Prandtl-Ishlinskii operators H and C. For implementation purposes the infinite-dimensional memory is approximated by a sufficiently high finite-dimensional memory. This means that the operators H and C are defined by the superposition of a finite number of elementary operators with local memory.

For the hysteresis operator, these elementary operators have to fulfill the Madelung rules. Suitable elementary operators are the linear play and stop operators, see, e.g., [6]. In the following, only the linear play operator is considered. The play operator P_{r_H} parametrized by the threshold value $r_H \in \mathbb{R}_0^+$ is defined as

$$\begin{aligned} \chi_H(t) &= P_{r_H}[\upsilon(t), \chi_H(t_j)] \\ &= \max\{\upsilon(t) - r_H, \min\{\upsilon(t) + r_H, \chi_H(t_j)\}\}, \ t_j < t \leq t_{j+1} \end{aligned} \tag{7}$$

with the initial consistency condition for $\chi_H(t_0) = \chi_{H0}$ given by

$$\chi_{H0} = \max\{\upsilon(t_0) - r_H, \min\{\upsilon(t_0) + r_H, \chi_{H0}\}\} \tag{8}$$

for piecewise monotonous input signals $\upsilon(t)$ with a monotonicity partition $t_0 \leq t_1 \leq ... \leq t_j < t \leq t_{j+1} \leq ... \leq t_N$. Hence, the appropriate operator equation is usually given in the form

$$\chi_H(t) = P_{r_H}[\upsilon, \chi_{H0}](t). \tag{9}$$

The finite-dimensional memory structure of the Prandtl-Ishlinskii hysteresis operator H is achieved by the weighted superposition of $n_H + 1$ elementary linear play operators such that

$$\varsigma_H(t) = H[\upsilon, \boldsymbol{\chi}_{H0}](t) = \sum_{i=0}^{n_H} w_{H,i}\chi_{H,i}(t) = \sum_{i=0}^{n_H} w_{H,i}P_{r_{H,i}}[\upsilon, \chi_{H0,i}](t), \tag{10}$$

with initial values $\boldsymbol{\chi}_{H0} = [\chi_{H0,0}, \chi_{H0,1}, \ldots, \chi_{H0,n_H}]^T$, the weights w_{Hi}, and the threshold values r_{Hi} with $i = 0, ..., n_H$ fulfilling the conditions

$$\sum_{i=0}^{n_H} w_{H,i} < \infty, \tag{11}$$

$$0 = r_{H,0} < r_{H,1} < r_{H,2} < ... < r_{H,n_H} < \infty, \tag{12}$$

whereas (11) ensures strong monotonicity in the branching behavior. In this representation the outputs of the elementary operators $\chi_{H,i}$ are also called the inner system states of the so-called threshold-discrete Prandtl-Ishlinskii hysteresis operator H.

As already mentioned before, a similar approach can be used in order to model the rate-dependent creep effects. Here, the elementary creep operator

$$\chi_C(t) = K_{r_C,a}[\upsilon, \chi_{C0}](t), \tag{13}$$

Post-print version of the article: J. Schröck, T. Meurer, and A. Kugi, "Control of a flexible beam actuated by macro-fiber composite patches: II. Hysteresis and creep compensation, experimental results", *Smart Materials and Structures*, vol. 20, no. 015016, pp. 1–10, 2011.
DOI: 10.1088/0964-1726/20/1/015016
The content of this post-print version is identical to the published paper but without the publisher's final layout or copy editing.

is defined by the solution of the nonlinear differential equation

$$\frac{\mathrm{d}}{\mathrm{d}t}\chi_C(t) - aP_{r_C}[\upsilon - \chi_C, 0](t) = 0 \tag{14}$$

with the play operator P_{r_C} and the initial condition $\chi_C(t_0) = \chi_{C0}$, see [15]. The elementary operator $K_{r_C,a}$ depends on the creep eigenvalue $a \in \mathbb{R}^+$ and on the threshold value r_C of the play operator. As shown in [14], the detected $\log(t)$-creep behavior can be reproduced by an unweighted superposition of m_C elementary creep operators with different creep eigenvalues a_j, $j = 1, ..., m_C$ but equal threshold value r_C, which results in the so-called elementary $\log(t)$-creep operator given by

$$\tilde{\varsigma}_C = \frac{1}{m_C}\sum_{j=1}^{m_C}\chi_{C,j}(t) = \frac{1}{m_C}\sum_{j=1}^{m_C}K_{r_C,a_j}[\upsilon, \chi_{C0,j}](t). \tag{15}$$

Finally, the model of the creep behavior with memory effect is given by a threshold-discrete Prandtl-Ishlinskii creep operator that is based on a number of n_C+1 elementary $\log(t)$-creep operators with different threshold values $r_{C,i}$, i.e.

$$\varsigma_C(t) = C[\upsilon, \boldsymbol{\chi}_{C0}](t) = \sum_{i=0}^{n_C} w_{C,i}\tilde{\varsigma}_{C,i} = \sum_{i=0}^{n_C}\frac{w_{C,i}}{m_C}\sum_{j=1}^{m_C}K_{r_{C,i},a_j}[\upsilon, \chi_{C0,i,j}](t), \tag{16}$$

with initial values $\boldsymbol{\chi}_{C0} = [\chi_{C0,1,1}, \chi_{C0,1,2}, \ldots, \chi_{C0,n_c,m_c-1}, \chi_{C0,n_c,m_c}]^T$ and

$$\sum_{i=0}^{n_C} w_{C,i} < \infty, \tag{17}$$

$$0 = r_{C,0} < r_{C,1} < r_{C,2} < ... < r_{C,n_C} < \infty, \tag{18}$$

In summary, the considered hysteresis and creep model (6) is given by two threshold-discrete Prandtl-Ishlinskii operators consisting of $(n_C + 1)m_C + n_H + 1$ inner state variables $\boldsymbol{\chi} = [\chi_{H,0}, ..., \chi_{H,n_H}, \chi_{C,0,1}, ..., \chi_{C,n_C,m_C}]^T$ that are determined by $n_H + n_C + 2$ threshold parameters $\mathbf{r} = [r_{H,0}, ..., r_{H,n_H}, r_{C,0}, ..., r_{C,n_C}]^T$, m_C creep eigenvalues $\mathbf{a} = [a_1, ..., a_{m_C}]^T$ and $n_H + n_C + 2$ weighting parameters $\mathbf{w} = [w_{H,0}, ..., w_{H,n_H}, w_{C,0}, ..., w_{C,n_C}]^T$.

For the compensator design the inverse hysteresis and creep operator $\upsilon(t) = W^{-1}[\varsigma](t)$, which is defined by the implicit operator equation

$$\upsilon(t) = H^{-1}[\varsigma - C[\upsilon]](t), \tag{19}$$

is required. The existence and uniqueness of this inverse operator is shown in [16].

For the real-time implementation of the compensator, a time-discrete solution based on time-discrete hysteresis and creep Prandtl-Ishlinskii operators is derived in the following. Assuming a staircase-shaped input signal that is constant between the sampling instances $(k-1)T_s$ and kT_s with sampling time T_s the time-discrete play operator $\hat{P}_{r_H}$ and the time-discrete elementary creep operator $\hat{K}_{r_C,a}$ are given by [15]

$$\begin{aligned}\chi_H^k &= \hat{P}_{r_H}[\upsilon^k, \chi_H^{k-1}] = \max\{\upsilon^k - r_H, \min\{\upsilon^k + r_H, \chi_H^{k-1}\}\},\\ \chi_C^k &= \hat{K}_{r_C,a}[\upsilon^{k-1}, \chi_C^{k-1}] = \chi_C^{k-1} + (1-\exp^{-aT_s})\hat{P}_{r_C}[\upsilon^{k-1} - \chi_C^{k-1}, 0].\end{aligned} \tag{20}$$

Post-print version of the article: J. Schröck, T. Meurer, and A. Kugi, "Control of a flexible beam actuated by macro-fiber composite patches: II. Hysteresis and creep compensation, experimental results", *Smart Materials and Structures*, vol. 20, no. 015016, pp. 1–10, 2011.
DOI: 10.1088/0964-1726/20/1/015016

Note that the output of $\hat{K}_{r_C,a}$ at the time instance k depends only on the state of the rate-dependent part χ_C^{k-1} and on the input υ^{k-1} at time instance $(k-1)T_s$. From this it follows that the compensator in its time-discrete form

$$\upsilon^k = \hat{H}^{-1}[\varsigma^k - \hat{C}[\upsilon^{k-1}]] \tag{21}$$

is no longer an implicit operator equation. It can be shown that under the assumption that the Prandtl-Ishlinskii hysteresis operator H has a strong monotonicity in the branching behavior (11) the appropriate inverse operator H^{-1} exists uniquely and is again a Prandtl-Ishlinskii operator, see [17]. This also holds true for the time discrete form of the inverse hysteresis operator $\upsilon^k = \hat{H}^{-1}[\varsigma, \chi'_{H0}]^k$, where the weights w'_{Hi}, thresholds r'_{Hi}, and initial values χ'_{H0i} can be calculated by simple transformation rules from the appropriate values of the original operator, see, e.g., [18]

$$\begin{array}{ll} r'_{H,j} & = w_{H,0} r_{H,j} + \sum_{i=1}^{j} w_{H,i}(r_{H,j} - r_{H,i}), \\ w'_{H,0} & = \frac{1}{w_{H,0}}, \quad w'_{H,j} = -\frac{w_{H,j}}{(\sum_{i=0}^{j} w_{H,i})(\sum_{i=0}^{j-1} w_{H,i})}, \\ \chi'_{H0,j} & = (\sum_{i=0}^{j} w_{H,i})\chi_{H0,j} + \sum_{i=j+1}^{n} w_{H,i}\chi_{H0,i}. \end{array} \tag{22}$$

Hence, after the identification of the hysteresis and creep parameters represented by the weights, the thresholds and the creep eigenvalues the output signal of the compensator v_k can be directly calculated by means of (21).

3.2. Determination of hysteresis and creep parameters

As shown in [14] the identification problem of the hysteresis and creep model (6) can be solved by the following procedure. After an appropriate choice of the model order represented by n_H, n_C, and m_C, the thresholds are calculated according to

$$r_{H,i} = \frac{r_{max}}{n_H + 1} i, \ i = 0, ..., n_H, \qquad r_{C,i} = \frac{r_{max}}{n_C + 1} i, \ i = 0, ..., n_C, \tag{23}$$

where r_{max} is set to the maximum value of the absolute input signal, i.e. $r_{max} = \max|\upsilon(t)|$. In order to reproduce the linear creep response shown in figure 9, the creep eigenvalues of the model have to be exponentially distributed [14], i.e.

$$a_j = \frac{1}{10^j T_s}, \ j = 1, ..., m_C. \tag{24}$$

The determination of the weights $\mathbf{w} = [w_{H,0}, ..., w_{H,n_H}, w_{C,0}, ..., w_{C,n_C}]^T$ relies on the minimization of the least-squares measure based on the output error constrained by the linear inequality constraints (11) and (17), i.e.

$$\begin{array}{l} \min\limits_{\mathbf{w}} \frac{1}{2} \int\limits_{t_s}^{t_e} (W[\upsilon](t) - \varsigma(t))^2 \mathrm{d}t, \\ \text{subject to } \sum\limits_{i=0}^{n_H} w_{H,i} < \infty, \ \sum\limits_{i=0}^{n_C} w_{C,i} < \infty. \end{array} \tag{25}$$

On the assumption that the error model is non-redundant in the weights and all elementary operators get excited during the identification process by choosing an appropriate input signal the constrained minimization problem is strongly convex and has a unique solution [19].

Post-print version of the article: J. Schröck, T. Meurer, and A. Kugi, "Control of a flexible beam actuated by macro-fiber composite patches: II. Hysteresis and creep compensation, experimental results", *Smart Materials and Structures*, vol. 20, no. 015016, pp. 1–10, 2011.
DOI: 10.1088/0964-1726/20/1/015016
The content of this post-print version is identical to the published paper but without the publisher's final layout or copy editing.

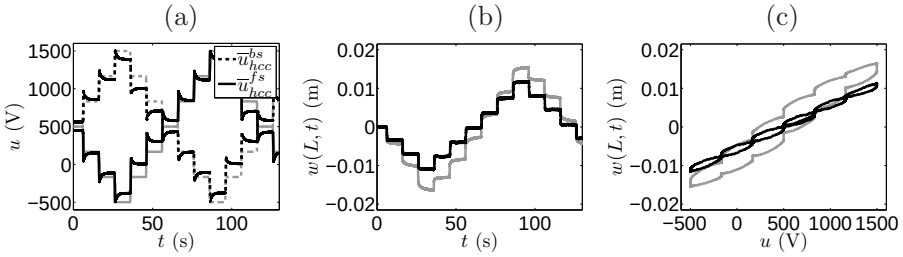

Figure 10. Effect of the compensator in comparison to figure 3 (represented by grey lines). (a) Voltage signals generated by the compensator for the patch actuator on the front and back side, $\overline{u}_{hcc}^{fs}(t)$ and $\overline{u}_{hcc}^{bs}(t)$, respectively, (b) position of the beam's tip w, (c) compensated hysteresis and creep behavior w/u.

4. Experimental results

In a first step, the effectivity of the hysteresis and creep compensator is verified by measurements. Afterwards, it is shown that the combination of this compensator with the feedforward control design as proposed in the companion paper [1] allows to perform accurate highly dynamic open-loop tracking control.

4.1. Hysteresis and creep compensation

The model order of the hysteresis and creep model is chosen in form of $n_H + 1 = 12$ elementary hysteresis operators and $n_C + 1 = 12$ elementary $\log(t)$-creep operators with $m_C = 5$ creep eigenvalues. By applying a periodic staircase voltage signal as depicted in figure 3 (a) with the overall amplitude being sequentially reduced in each period, the weights $\mathbf{w}$ are determined by minimization of the least-squares error (25). The application of the resulting compensator (21) shows that this approach almost completely eliminates the actuator nonlinearities, see figure 10. For comparison reasons, the same scenario as presented in figure 3 is utilized, whereas the results without hysteresis and creep compensation are depicted by the grey lines. Hence, figure 10 (a) allows to compare the prescribed voltage signals (grey) with voltages generated by the compensator (black). Obviously, the nonlinear actuator behavior is eliminated by adaption of the voltage step height and by the decreasing voltage peaks at the beginning of each step. Clearly, apart from some minor variations this results in a linear relation between the beam's tip deflection and the prescribed voltage signal.

4.2. Model identification

For the realization of the feedforward control design proposed in [1] the determination of the system parameters of the MFC-actuated cantilever is of decisive importance. The experimental setup includes a cantilever beam structure consisting of pre-impregnated glass fibre material of dimension $L = 0.22\,\mathrm{m}$, $b_c = 0.075\,\mathrm{m}$, and $h_c = 0.7 \times 10^{-3}\,\mathrm{m}$. On each side of the beam an MFC patch actuator (type $M8557P1$, see [20]) with an active area of dimension $L_p = 85 \times 10^{-3}\mathrm{m}$, $b_p = 57 \times 10^{-3}\mathrm{m}$, $h_p = 3 \times 10^{-4}\mathrm{m}$, and electrode

Post-print version of the article: J. Schröck, T. Meurer, and A. Kugi, "Control of a flexible beam actuated by macro-fiber composite patches: II. Hysteresis and creep compensation, experimental results", *Smart Materials and Structures*, vol. 20, no. 015016, pp. 1–10, 2011.
DOI: 10.1088/0964-1726/20/1/015016
The content of this post-print version is identical to the published paper but without the publisher's final layout or copy editing.

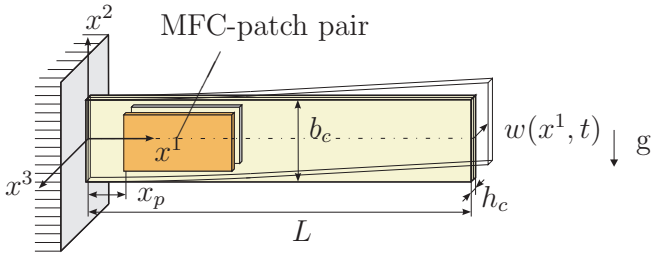

Figure 11. Schematics of the considered flexible beam actuated by one pair of MFC patches.

spacing $e_s = 5 \times 10^{-4}\,\mathrm{m}$, is bonded symmetrically at a distance of $x_p = 32.5 \times 10^{-3}\mathrm{m}$ from the clamped edge (cf. figure 11). The beam's tip deflection is measured by a laser sensor based on the triangulation measurement principle. The measurements and the implementation of the feedforward control concept are realized using the real-time control board DS1103 of dSPACE with a sampling time of $T_s = 0.2\,\mathrm{ms}$. The power supply is provided by two high-voltage four-quadrant power amplifiers PA05039 of Trek Inc. [20]. With respect to the Hammerstein-like model the linear flexible beam model is given by

$$\begin{aligned}&\mu(x^1)\partial_t^2 w + \gamma^e(x^1)\partial_t w + \partial_{x^1}^2\left(\Lambda(x^1)\partial_{x^1}^2 w + \gamma^i(x^1)\partial_t\partial_{x^1}^2 w\right)\\&= -2u\Gamma_p\partial_{x^1}^2\Omega(x^1),\end{aligned} \tag{26}$$

together with the respective boundary conditions (BCs) at the clamped end ($x^1 = 0$) and at the free end ($x^1 = L$) following as

$$\left.\begin{aligned}&w = 0,\ \partial_{x^1} w = 0, && \text{for} \quad x^1 = 0\\&\Lambda_c\partial_{x^1}^2 w + \gamma_c^i\partial_t\partial_{x^1}^2 w = 0,\\&\Lambda_c\partial_{x^1}^3 w + \gamma_c^i\partial_t\partial_{x^1}^3 w = 0,\end{aligned}\right\} \quad \text{for} \quad x^1 = L. \tag{27}$$

Here, $\mu(x^1) = A_c\rho_c + 2A_p\rho_p\Omega(x^1)$ denotes the mass per unit length, $\Lambda(x^1) = \Lambda_c + 2\Lambda_p\Omega(x^1)$ the stiffness, $\gamma^e(x^1) = \gamma_c^e + 2\gamma_p^e\Omega(x^1)$ and $\gamma^i(x^1) = \gamma_c^i + 2\gamma_p^i\Omega(x^1)$ the viscous and Kelvin-Voigth damping coefficient, respectively, while $\Gamma_p = A_p(h_c + h_p)h_1^{11}/(2\beta_{11}e_s)$ summarizes some material parameters and $\Omega(x^1) = [h(x^1 - x_p) - h(x^1 - x_p - L_p)]$ with the Heaviside function $h(\cdot)$ specifies the placement of the MFC-patch pair. For further details and the derivation of the equations of motion the reader is referred to [1].

In order to account for model uncertainties due to an anisotropic behavior of the material and due to the neglected adhesive layers between the MFC patches and the beam material a parameter identification has to be performed. Note that in general this is not a trivial task since some parameters of the model will be significantly influenced by the hysteresis and creep effects of the MFC actuators. However, the application of the developed compensator, which cancels the nonlinear effects, allows to determine the parameters of the linear beam model by means of standard identification techniques. Measurements demonstrate that the step response of the hysteresis and creep compensated MFC-actuated beam represents the typical behavior of a linear beam

Post-print version of the article: J. Schröck, T. Meurer, and A. Kugi, "Control of a flexible beam actuated by macro-fiber composite patches: II. Hysteresis and creep compensation, experimental results", *Smart Materials and Structures*, vol. 20, no. 015016, pp. 1–10, 2011.
DOI: 10.1088/0964-1726/20/1/015016
The content of this post-print version is identical to the published paper but without the publisher's final layout or copy editing.

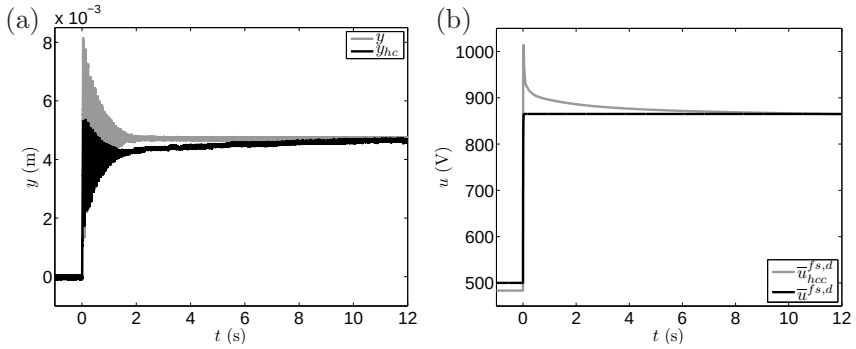

Figure 12. (a) Step response with and without hysteresis and creep compensation, y_{hc} and y, respectively. (b) Input voltages of the patch actuator on the front side of the beam with and without compensation, $\overline{u}_{hcc}^{fs,d}(t)$ and $\overline{u}^{fs,d}(t)$, respectively.

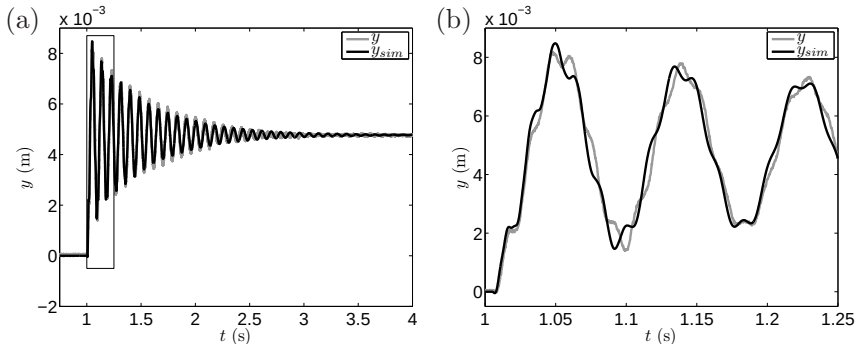

Figure 13. (a) Comparison of measured y and simulated step response y_{sim}. (b) Detailed view of the time period $[1, 1.25]$ s

model, as is illustrated in figure 12 (a). Clearly, the creep effects are fully canceled out by application of the voltage signal generated by the compensator, which is shown in figure 12 (b) for the patch on the front side of the beam $\overline{u}_{hcc}^{fs,d}(t)$. This allows the identification of the system parameters according to $\gamma_c^e = 10^{-3}\,\mathrm{kg/(sm)}$, $\gamma_c^i = 5.1 \times 10^5\,\mathrm{kgm^3/s}$, $\gamma_p^e = 2.93\,\mathrm{kg/(sm)}$, $\gamma_p^i = 10^6\,\mathrm{kgm^3/s}$, $Y_c = 17.06 \times 10^9\,\mathrm{Pa}$, $c_p^{1111} = 31.97 \times 10^9\,\mathrm{Pa}$, $\rho_c = 1187.6\,\mathrm{kg/m^3}$, $\rho_p = 4761.4\,\mathrm{kg/m^3}$, and $a_1^{11}/\beta_{11} = 11.88\,\mathrm{As/m^2}$ by minimizing the mean square error between a measured and a simulated step response based on the finite-dimensional approximation with $n = 15$ basis functions [1]. As illustrated in figure 13, these parameter values result in an excellent agreement of the measured and the simulated step responses of the MFC-actuated cantilever.

4.3. Feedforward tracking control

Finally, the tracking behavior achieved by the feedforward control proposed in [1] combined with the hysteresis and creep compensation is investigated in experiments. For this, the parametrization of the finite-dimensional model [1, Section 3.2.] is evaluated with $n = 15$ basis functions. The nominal input voltage $\overline{u}^{fs/bs,d}(t) = u_0 \pm u^d(t)$, with

Post-print version of the article: J. Schröck, T. Meurer, and A. Kugi, "Control of a flexible beam actuated by macro-fiber composite patches: II. Hysteresis and creep compensation, experimental results", *Smart Materials and Structures*, vol. 20, no. 015016, pp. 1–10, 2011.
DOI: 10.1088/0964-1726/20/1/015016
The content of this post-print version is identical to the published paper but without the publisher's final layout or copy editing.

$u^d(t)$ determined from the proposed input parametrization [1, Eq. (33)], is calculated based on the same flat output trajectory $z^d(t)$ as already considered in the simulation scenario in [1], i.e.

$$z^d(t) = \begin{cases} z_0^d, & t < 0 \\ z_0^d + \frac{z_T^d}{2}\left(1 + \tanh\left(\frac{2\left(\frac{2t}{T}-1\right)}{\left(\frac{4t}{T}\left(1-\frac{t}{T}\right)\right)^{\sigma}}\right)\right), & t \in [0, T] \\ z_0^d + z_T^d, & t > T \end{cases} \tag{28}$$

where the slope and the transition time of this function is chosen by $\sigma = 1.1$ and $T = 0.75$ ms, respectively. Note that the first eigenfrequency of the considered beam structure is at about 12 Hz such that the transition time T is smaller than the time constant corresponding to this eigenfrequency. As depicted in figure 14 (a) and (b) measurements of the beam's tip displacement show a very accurate realization of prescribed highly dynamic rest-to-rest trajectory from $y^d(t_0) = 0$ m to $y^d(t_0 + T) = 0.01$ m without excitation of spurious oscillations. Of course, this result strongly depends on the correct compensation of the hysteresis and creep effects. Figures 14 (c) and (d) compare the nominal input voltage $\overline{u}^{fs,d}(t)$ to the pre-processed output voltage $\overline{u}_{hcc}^{fs,d}(t)$ of the compensator, which is finally applied to the MFC actuator on the front side of the beam. In particular after completion of the transition phase the evolution of the voltage signal $\overline{u}_{hcc}^{fs,d}(t)$ shows the contribution of the creep compensation that is necessary to obtain a constant drift free tip displacement of the beam. It has to be emphasized that no feedback control is involved but only the determined feedforward control with hysteresis and creep compensation is applied to the MFC patch actuators.

5. Conclusion and outlook

This contribution presents an operator based compensator design for an MFC-actuated flexible beam. A detailed analysis of the inherent hysteresis and creep behavior of the considered MFC patch actuators shows that these nonlinearities can be efficiently modeled by means of a Prandtl-Ishlinskii operator. Based on a Hammerstein-like model with the hysteresis and creep operator at the input connected in series with a linear infinite-dimensional beam model the compensator directly results from the inverse operator. The pleasing property that the inverse operator is again a Prandtl-Ishlinskii operator and the fact that the weight and threshold parameters of the inverse operator can be directly determined by simple transformation rules from those of the original operator makes this approach very suitable for an automated identification procedure in a realtime environment. Measurements prove that this compensator design allows to cancel the nonlinearities induced by the hysteresis and creep effects of the MFC-patch actuators. Additionally, the applicability of the motion planning and feedforward control design proposed in [1], which is based on an infinite-dimensional hysteresis and creep compensated model, is validated by experimental results. Measurements show that highly dynamic rest-to-rest trajectories for the beam's tip deflection can be realized with high tracking accuracy.

Post-print version of the article: J. Schröck, T. Meurer, and A. Kugi, "Control of a flexible beam actuated by macro-fiber composite patches: II. Hysteresis and creep compensation, experimental results", *Smart Materials and Structures*, vol. 20, no. 015016, pp. 1–10, 2011.
DOI: 10.1088/0964-1726/20/1/015016
The content of this post-print version is identical to the published paper but without the publisher's final layout or copy editing.

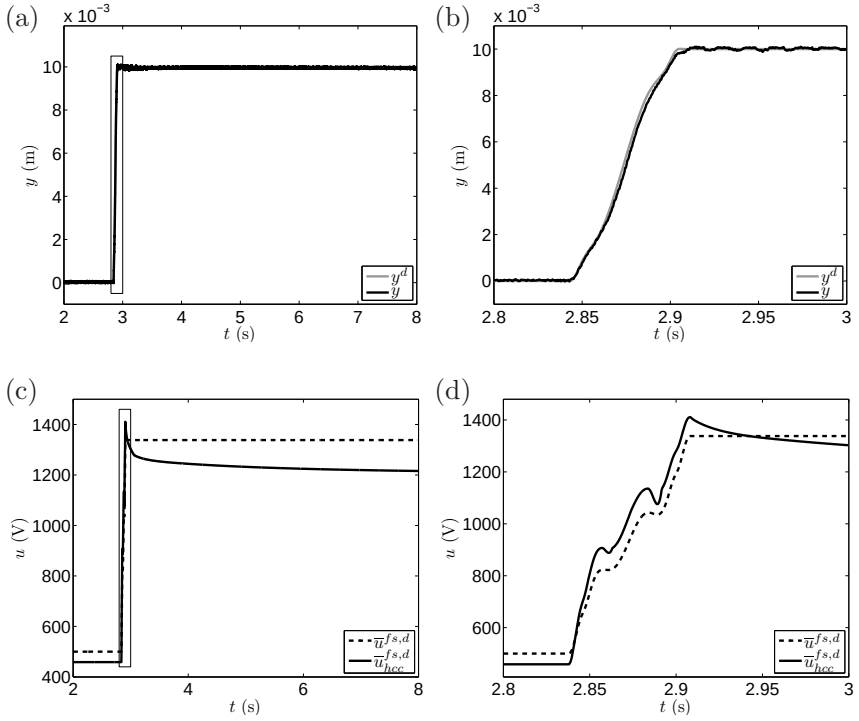

Figure 14. Experimental results for the application of the flatness-based feedforward control to the flexible cantilevered beam with two MFC patch actuators. (a) Desired (gray) and measured (black) output trajectory. (c) Input voltage $\overline{u}^{fs,d}(t) = u_0 - u^d(t)$ with $u_0 = 500\,\mathrm{V}$ applied to the patch actuator on the front side: nominal input $\overline{u}^{fs,d}(t)$ (dashed line) and input after the pre-processing by the hysteresis and creep compensation $\overline{u}^{fs,d}_{hcc}(t)$ (solid line). (b),(d) Detailed views of the time period $[2.8, 3]$ s.

Future research is devoted to augment the feedforward control with feedback control within the so-called two-degrees-of freedom control concept (see, e.g., [21]) in order to be able do suppress disturbances acting on the beam structure.

References

[1] J. Schröck, T. Meurer, and A. Kugi, "Flexible beam actuated by macro-fiber composite patches–Part I: Modelling and feedforward trajectory control," *SIAM Smart Material and Structures*, 2010, submitted.

[2] R. B. Williams, G. Park, D. J. Inman, and W. K. Wilkie, "An overview of composite actuators with piezoceramic fibers," *Proc. of 20th Int. Modal Analysis Conf.*, February 4-7 2002.

[3] H. Janocha, Ed., *Adaptronics and Smart Structures*, 2nd ed. Berlin, Heidelberg, New York: Springer, 2007.

[4] H. T. Banks, R. C. H. Smith, and Y. Wang, *Smart Material Structures: Modelling, Estimation and Control*. Paris (F): John Wiley & Sons, 1996.

[5] M. Brokate, *Hysteresis and phase transitions*. New York, Berlin, Heidelberg: Springer, 1996.

[6] A. Visintin, *Differential Models of Hysteresis*. New York, Berlin, Heidelberg: Springer, 1994.

[7] A. Kugi, D. Thull, and K. Kuhnen, "An infinite-dimensional control concept for piezoelectric structures with complex hysteresis," *Structural Control and Health Monitoring*, vol. 13, no. 6, pp. 1099–1119, 2006.

Post-print version of the article: J. Schröck, T. Meurer, and A. Kugi, "Control of a flexible beam actuated by macro-fiber composite patches: II. Hysteresis and creep compensation, experimental results", *Smart Materials and Structures*, vol. 20, no. 015016, pp. 1–10, 2011.
DOI: 10.1088/0964-1726/20/1/015016
The content of this post-print version is identical to the published paper but without the publisher's final layout or copy editing.

[8] K. Kuhnen, "Modeling, identification and compensation of complex hysteretic nonlinearities - a modified Prandtl-Ishlinskii approach," *European J. of Control*, vol. 9, no. 4, pp. 407–418, 2003.

[9] P. Haupt, *Continuum Mechanics and Theory of Materials*. Berlin, Heidelberg, New York: Springer, 2002.

[10] C. V. Newcomb and I. Flinn, "Improving the linearity of piezoelectric ceramic actuators," *Electronics Letters*, vol. 18, pp. 442–444, 1982.

[11] H. Janocha, M. Klein, and K. Kuhnen, "Simultane Messung charakteristischer Kenngrößen von Piezoaktoren im Großsignalbetrieb," *tm - Technisches Messen*, vol. 69, no. 9, pp. 399–403, 2002.

[12] K. Kuhnen, *Kompensation komplexer gedächtnisbehafteter Nichtlinearitäten in Systemen mit aktiven Materialien*. Aachen (D): Shaker, 2008.

[13] E. Madelung, "Über Magnetisierung durch schnell verlaufende Ströme und die Wirkungsweise des Rutherford-Marconischen Magnetdetektors," *Ann. Phys.*, vol. 17, pp. 891–890, 1905.

[14] K. Kuhnen, "Modeling, identification and compensation of complex hysteretic and log(t)-type creep nonlinearities," *J. Control and Intelligent Systems*, vol. 33, no. 2, pp. 134–147, 2005.

[15] K. Kuhnen and P. Krejci, "Compensation of complex hysteresis and creep effects in piezoelectrically actuated systems - a new Preisach modeling approach," *IEEE Transactions on Automatic Control*, vol. 54, no. 3, pp. 537–550, 2009.

[16] P. Krejci and K. Kuhnen, "Existence, uniqueness and L_∞-stability of the Prandtl-Ishlinskii hysteresis and creep compensator," *European J. of Control*, vol. 14, pp. 409–417, 2008.

[17] P. Krejci, *Hysteresis, Convexity and Dissipation in Hyperbolic Equations*. Gakkotosho, Tokyo (J): Gakuto Int. Series Math. Sci. & Appl., 1996, vol. 8.

[18] P. Krejci and K. Kuhnen, "Inverse control of systems with hysteresis and creep," *IEEE Proceedings–Control Theory and Applications*, vol. 148, no. 3, pp. 185–192, 2001.

[19] K. Kuhnen and P. Krejci, "Identification of linear error-models with projected dynamical systems," *Mathematical and Computer Modelling of Dynamical Systems*, vol. 10, no. 1, pp. 59–91, 2004.

[20] Datasheet, http://www.smart-material.com.

[21] T. Meurer, D. Thull, and A. Kugi, "Flatness–based tracking control of a piezoactuated Euler–Bernoulli beam with non–collocated output feedback: theory and experiments," *Int. J. Control*, vol. 81, no. 3, pp. 473–491, 2008.

Post-print version of the article: J. Schröck, T. Meurer, and A. Kugi, "Control of a flexible beam actuated by macro-fiber composite patches: II. Hysteresis and creep compensation, experimental results", *Smart Materials and Structures*, vol. 20, no. 015016, pp. 1–10, 2011.
DOI: 10.1088/0964-1726/20/1/015016